Unveiling Brain Tumors: An Approach Using Graph Theory in Medical Imaging

Nihaas Reddy Ravula, Dheeraj Reddy Balasani, Aishwarya Sudhir, Kartheek Reddy T, Asha Ashok, Manjushanair
Department of Computer Science and Engineering, Amrita School of Computing,
Amrita Vishwa Vidyapeetham, Amritapuri, Kerala India
ravulanihaasreddy@gmail.com, dheerajreddy10869@gmail.com, aiswaryasudhir24@gmail.com,
kartheekvishal26@gmail.com, ashaashok@am.amrita.edu, manjushanair@am.amrita.edu

***Abstract*—This research provides a novel method for classifying brain tumors in MRI images that combines graph neural networks (GNN) with convolutional neural networks (CNN). Preprocessed MRI images are translated into graphical representations to capture spatial dependencies and feature extraction is facilitated by transfer learning with CNN architectures. The core model employs a lightweight network (GAT) to reveal information in network connections, resulting in a valuable learning experience for tumor classification. GAT employs a tracking strategy to choose input from neighboring individuals, hence enhancing the model's capacity to detect correlations in visual patterns. To better comprehend data features and representations, use qualitative data analysis and visualization tools. Three versions of this model were created and tested, namely VGG16, DenseNet121 and ResNet18 each based on a different previous CNN design. The accuracies range from 65-80% where VGG showed better accuracy. Overall, the hybrid method shows good potential for brain tumor classification in MRI scans.**

A. keywords

Convolutional Neural Networks(CNN), Graph Attention network(GAT), Graph convolutional network(GCN), Graph neural network(GNN), brain tumor classification(BTC)

I. Introduction

Brain tumors are anomalies that appear in the complex structure of the brain which has many physical and cognitive impacts on the patients. Clinicians conventionally use medical imaging techniques and manual examinations of the images for BTC. Conventional methods are susceptible to errors and depend on the competency of the examiner. It may overlook small changes that indicate the existence of tumors. Accurate and early discovery of brain tumor instances is critical to successful treatment and a better patient prognosis. This necessity has accelerated the development of computer-assisted detection systems, which provide healthcare workers with sophisticated diagnostic capabilities. One such innovation is the use of graph theory, a powerful approach for analyzing the intricate interconnections and patterns found in medical pictures, particularly in MRI and CT scans of the brain. Successful use of graph-based analysis on medical images can aid in computer-aided diagnostics for a range of disorders. There are new explorations like the use of Generative Adversarial Networks(GAN) for pre-training deep networks on the data to enhance the capability of the model to capture complex patterns and variations [1]. Interest in hybrid approaches combining deep networks with other computing methods is rising, like MedNet, a CNN model specifically designed for medical imaging [2]. The hybrid approaches bring in new ideas and improve accuracy [3]. Many previous studies also show integrating deep learning techniques with emerging technologies like the Internet of Things (IoT) for tumor classification like a CNN-based multi-class classification approach that offers automated diagnosis but also being prone to overfitting [4]. Some also focused on building a platform for understanding the working of tumors like a study where they focused on doing a 3D scaffold-based model for glioma stem cells providing a platform for drug testing that mimics the environment of the brain tumor [5]. Image enhancements and extensive data augmentation techniques are also done to refine the classification of tumors [6] [7]. There is also an AI-based model for BTC [8]. However, the effectiveness of model relies on how vast and diverse the training data is. Poor generalization to new, unseen data.

II. Materials and Methods

A. Dataset

MRI images were gathered from Kaggle which contain approximately 3264 images. The MRI , T1, T2 and FLAIR type 35 presented in this document are a combination of different patients and are generally divided into 4 groups: glioma tumor, meningioma tumor, no tumor, and pituitary tumor shown in Figure[1]. There are 394 images in test and 2700 images in train datasets. The different classes of the tumor are shown in Fig[1]

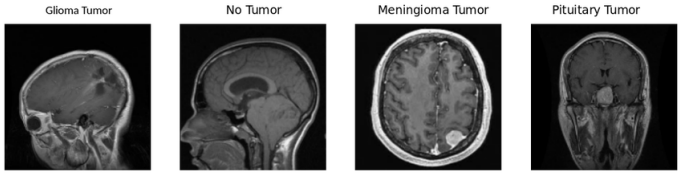

Fig. 1: Brain tumor classes in the dataset

B. Method

The study combines GNN and CNN to model the spatial information in MRI images effectively. By treating MRI as images, overcomes the limitations of regular pixel grid representation, allowing us to capture spatial dependencies and contextual relationships between pixels or areas. The images are preprocessed with resizing, normalization and so on. Image augmentation is performed like random cropping, translation, and Horizontal flip for the model input resolution. The CNN models are used to get the high-level features from the input images. These features capture complex patterns. The three variations are used to get the optimal one for the task: GAT-VGG16: Uses a pre-trained VGG-16 network for feature extraction with two GAT layers.

GAT-Densenet121: uses a pre-trained DenseNet-121 network, known for its efficient feature reuse along with two GAT layers.

GAT-Resnet18: Integrates a pre-trained ResNet-18 network, aiming to benefit from residual connections along with two GAT layers.

The graph is Constructed from the extracted feature maps. Each special region within the feature maps is treated as a node in the graph and edges are established between nodes based on their proximity in the feature space for which the K-nearest neighbour approach is used Where each node is connected to its k Most similar neighbors. The graph structure effectively captures the spatial relationships between the image regions.

In this research work, graph attention networks is used as the core GNN layers which use attention mechanisms to calculate the contributions of different neighboring nodes thereby allowing the model to focus on relevant information for the classification task. At last, the region-level class scores are aggregated from the GCN layers to obtain an image-level prediction.

III. Implementation

A. Data preprocessing and analysis

The data preprocessing begins for quality and consistency. It involves image resizing to the input resolution and normalization. Image augmentation includes random cropping, horizontal flipping and scaling which are applied to the dataset for the model's generalization capability.

Data analysis was conducted to gain insights into the characteristics of the dataset. Bar graphs are used to display the distribution of tumor categories in train and test datasets as shown in Fig[2]. The analysis gives information about the balance of classes and data structure which can also help in identifying any potential anomalies.

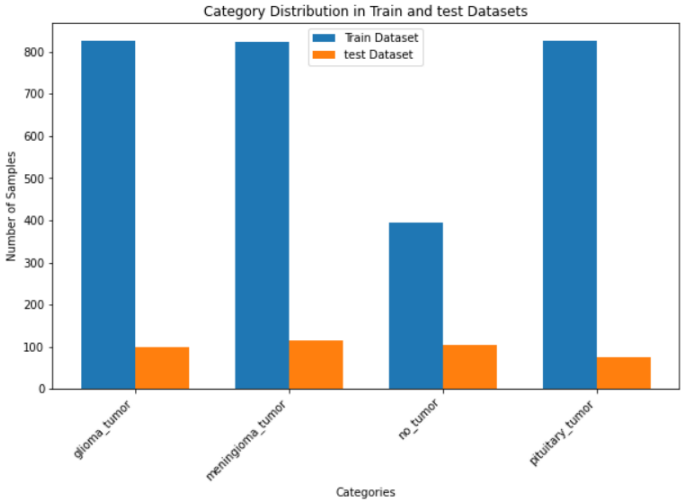

Fig. 2: Distribution in Training and Testing Datasets

IV. Model Architecture

The models share a common structure:

- Feature Extraction: The VGG16, ResNet18, or DenseNet121 models extract high-level features from the input brain MRI images. These features capture complex visual patterns learned from large-scale image datasets, serving as informative representations for subsequent analysis.
  - VGG-16:The network architecture operates on 224 x 224 RGB images, initially subjecting them to a pre-processing step involving mean subtraction for RGB value normalization. It comprises multiple stacks of convolutional layers, each stack featuring several convolutional layers with 3 x 3 receptive fields. These stacks vary in the number of filters per layer, with the first two stacks housing 64 filters, the third consisting of three layers with 256 filters, and the final two stacks containing three layers each with 512 filters. The GAT layers capture the contextual relationships between nodes in the graph, allowing for adaptive feature learning based on attention mechanisms. To downsample feature maps and reduce computational complexity, max-pooling is employed after every two convolutional layers, utilizing 2 x 2-pixel regions with a stride of 2 pixels. This pooling operation effectively halves the size of the feature maps at each stage with the final output size of 7x7x512.

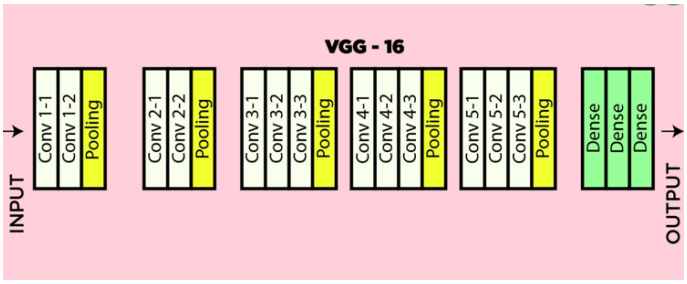

Fig. 3: VGG-16

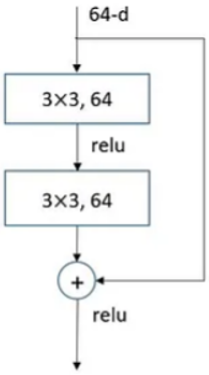

Fig. 5: Residual blocks

– DenseNet-121 The GAT_DenseNet integration goal is to increase the feature extraction by linking all layers and optimizing data flow across them. Unlike the conventional CNNs, the dense layers allow for strong feature propagation and reuse which helps in utilizing parameters. This combination helps to pass information across nodes through attention mechanisms which also improves the model's capacity to recognize the minute patterns and variations in tumor features.

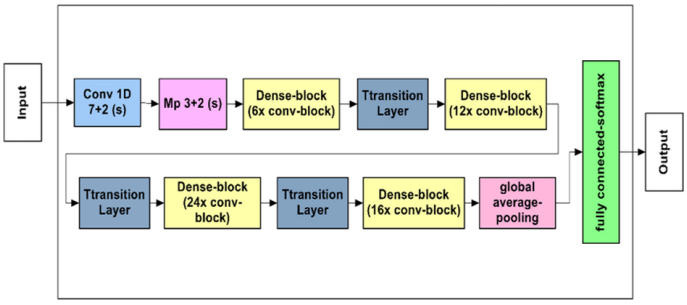

Fig. 4: DenseNet-121

– ResNet-18 GAT_ResNet, a combination of GAT and ResNet aims to make use of ResNet's residual connections(Fig[5]) which are known to mitigate the issue of vanishing gradient problems and incorporate them into GAT structure to train deeper networks. The several residual blocks with identity mappings and convolutional layers would make efficient feature extraction and pass them onto GAT layers.

- Graph Construction (`convert_graph`): The graph representations are constructed from the extracted feature maps. Each spatial region within the feature maps is treated as a node in the graph, and edges are established between nodes based on their proximity in the feature space following a k-nearest neighbors approach. This graph structure effectively captures the spatial relationships between image regions.
- Graph Attention Networks: Graph Attention Networks (GATs) are employed as the core GNN layers.Two GAT layers are utilized:
  – The first layer reduces the dimensionality of the features obtained from the pre-trained backbone model (512 for VGG16, 512 for ResNet18, and 1024 for DenseNet121) to a fixed dimension of 256.
  – The second layer produces node-level outputs in which channel numbers correspond to the number of classes in the task(e.g., four classes for glioma, meningioma, no tumor, and pituitary).
- Spatial Pooling and Classification: The final stage of the model involves aggregating the region-level class scores from the GCN layers to obtain an image-level prediction. Global mean pooling is utilized averaging the class scores across all image regions, to derive a final probability distribution over the possible tumor classes.

V. Results and Discussions

Lets compare the results between the three models using different evaluation metrics.

VI. Evaluation Metrics

A. Confusion Matrix

It shows how the predictions and the actual labels of the model for each class compare.

The ResNet, DenseNet, and VGG-16 matrices are shown below. Fig[6],[7], and [8] display the heatmaps in the same sequence.

As per Fig 6, the ResNet_GAT model performance is better when compared to Fig 7 in classifying no tumor and pituitary tumor with fewer misclassification.

According to Fig 7, the DenseNet_GAT model performed well at correctly classifying meningioma with 115 and no tumor cases with 104. The model seems to have difficulty differentiating between glioma and meningioma as there were 80 meningioma misclassified as glioma and 53 glioma misclassified as meningioma. There were 40 scans with no tumor misclassified as pituitary and 14 pituitary misclassified as no tumor.

Fig 8, VGG_GAT is similar to the other matrices, The Model seems to have difficulty in differentiating between glioma and meningioma(57 misclassification). There is a slight improvement in classifying both pituitary and non-tumor cases with fewer misclassifications.

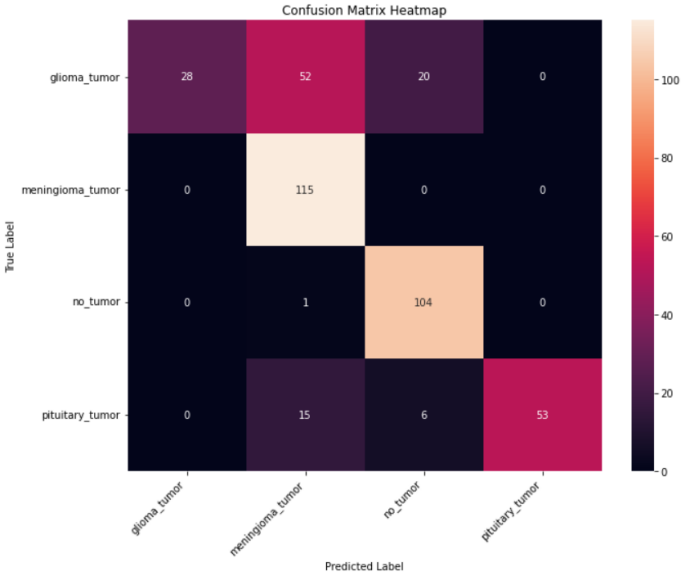

Fig. 6: ResNet_GAT

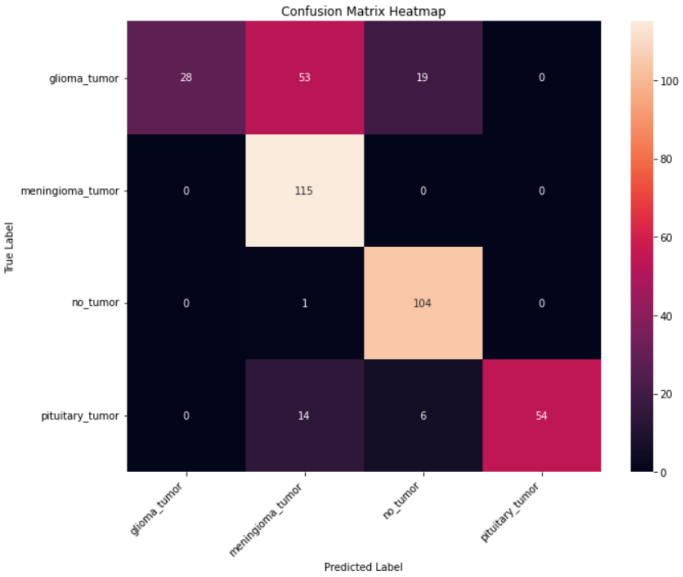

Fig. 7: DenseNet_GAT

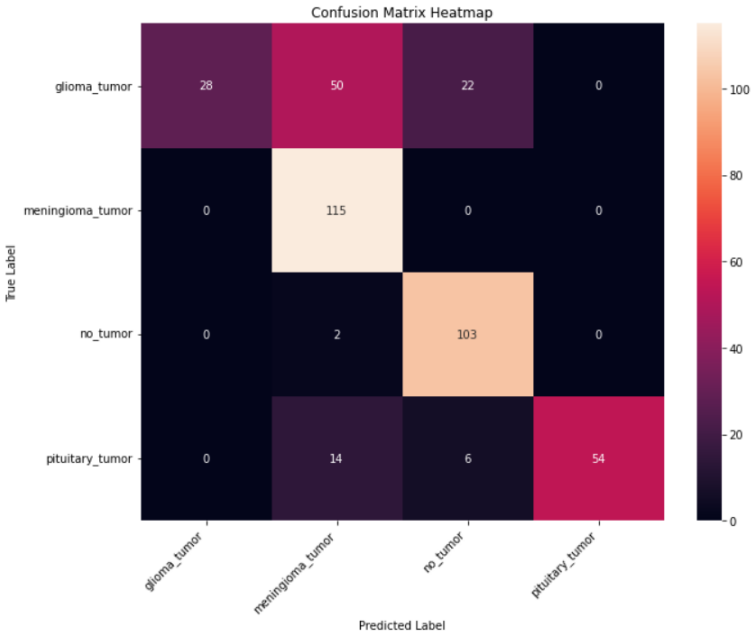

Fig. 8: VGG-16_GAT

B. ROC and AUC curves

It compares the true positive rate (correctly identified positive cases) on y-axis to the false positive rate (incorrectly identified negative cases) on x-axis at different thresholds. The area under curve(AUC) shows the model's overall performance at classification. They are depicted in Fig 9.

Comparing the three, it appears that all perform best at classifying pituitary tumor with AUC around 0.94 and worst at classifying glioma tumor with AUC ranging from 0.64 to 0.76. This can be due to pituitary tumors having more distinct imaging characteristics compared to other tumor types.

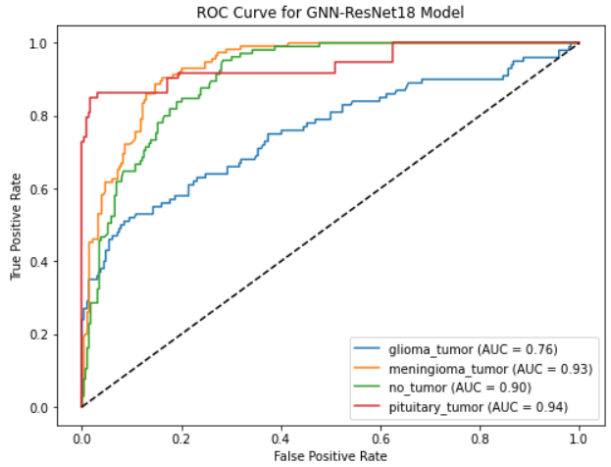

(a) ResNet_GAT

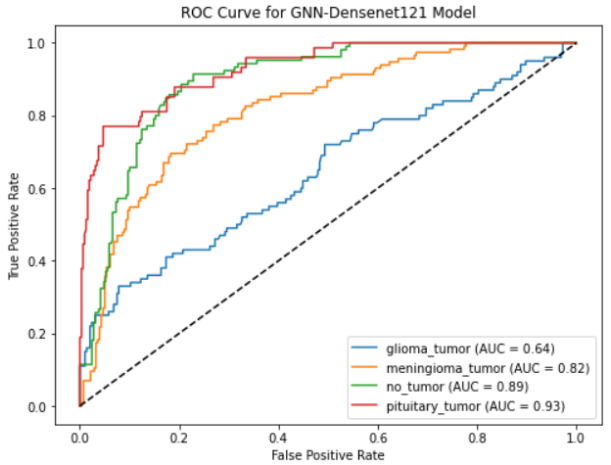

(b) DenseNet_GAT

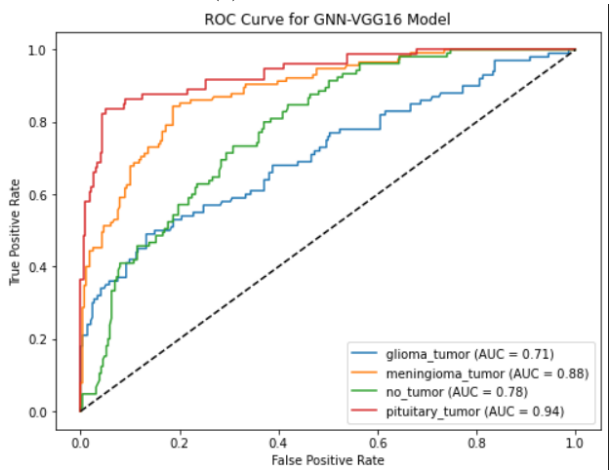

(c) VGG_GAT

Fig. 9: ROC curves for different architectures

C. Loss and Accuracy

Accuracy measures the proportion of correct predictions and loss is the difference between predicted and true labels. They are depicted in Fig 10. All three models have the potential to learn from the data where Fig 10b has high test accuracy and potentially lower overfitting.

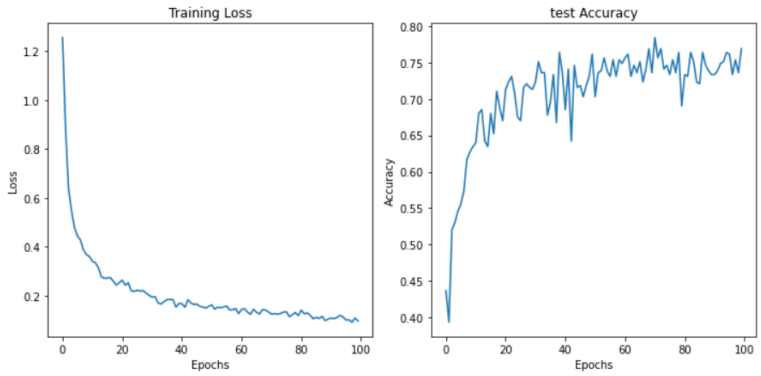

(a) ResNet_GAT

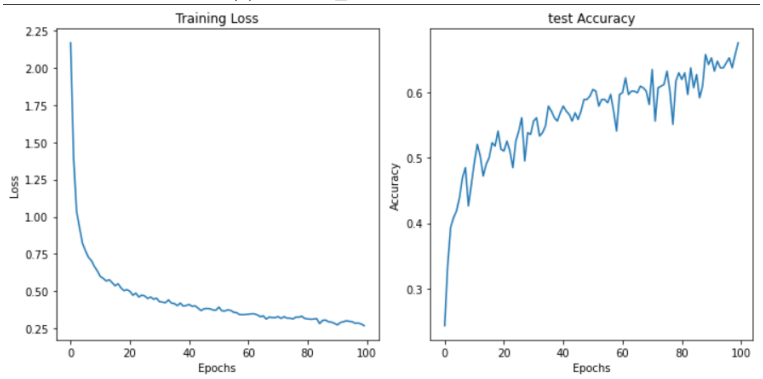

(b) Densenet_GAT

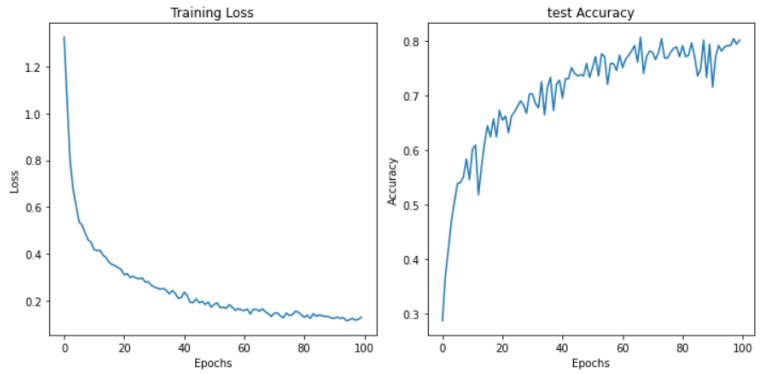

(c) VGG-16_GAT

Fig. 10: Loss and Accuracy curves for different architectures

D. Classification Report

In Classification reports, there are different performance metrics like Precision, Recall, and F1-score as shown in Tables I, II, III. ResNet_GAT (Table I) Seems to perform well with a weighted average of 0.73 and accuracy of 0.76 with class 1 having the highest recall. The model is good at identifying cases of class 1 and missing a significant portion of the cases of class 0. VGG_GAT(Table II) Performs well on all four classes with precision, recall and F1-score all being around 0.9 for each class which suggests that the model is good at identifying both positive and negative cases for all classes. DenseNet_GAT(Table III) Identifies class 1 and class 2 better

with good Recall. The model's Precision is high for class 0 and class 3 suggesting that all the model's predictions for these classes were correct.

	Precision	Recall	F1-score	Support
Class 0	1.00	0.28	0.44	100
Class 1	0.63	1.00	0.77	115
Class 2	0.80	0.99	0.89	105
Class 3	1.00	0.72	0.83	74
Accuracy			0.76	394
Macro Avg	0.86	0.75	0.73	394
Weighted Avg	0.84	0.76	0.73	394

TABLE I: ResNet_GAT

	Precision	Recall	F1-score	Support
Class 0	1.00	0.28	0.44	100
Class 1	0.64	1.00	0.78	115
Class 2	0.79	0.98	0.87	105
Class 3	1.00	0.73	0.84	74
Accuracy			0.76	394
Macro Avg	0.86	0.75	0.73	394
Weighted Avg	0.84	0.76	0.73	394

TABLE II: VGG_GAT

	Precision	Recall	F1-score	Support
Class 0	1.00	0.28	0.44	100
Class 1	0.63	1.00	0.77	115
Class 2	0.81	0.99	0.89	105
Class 3	1.00	0.73	0.84	74
Accuracy			0.76	394
Macro Avg	0.86	0.75	0.74	394
Weighted Avg	0.84	0.76	0.73	394

TABLE III: DenseNet_GAT

VII. Comparison and Findings

To understand the influence of switching from GCN to GAT, the performance of both models is compared while both of them use the same CNN architectures.

A. Comparison of GAT Models

GAT_VGG16: With GATs, the GAT_VGG16 model displays an accuracy of 79.69% from 71.31%. This signifies the GAT's ability to capture spatial dependencies which leads to enhanced feature representations.

GAT_Densenet121: The GAT_Densenet121 model increases the accuracy from 64.21% to 66.75%.

GAT_Resnet18: The GAT_Resnet18 model exhibits an increase in test accuracy with GATs, achieving an accuracy of 75.63% from 71.57%. Table IV and Table V show the accuracy of GAT and GCN models respectively.

B. Comparative Analysis

When both of them are compared, GAT models show a trend of increased accuracy across all of them. The attention mechanisms in GATs improve the propagation of information and feature learning which results in better classification performance.

TABLE IV: Test Accuracy for GAT Model

Model	Test Accuracy
GAT_VGG16	0.796954
GAT_Densenet121	0.667513
GAT_Resnet18	0.756345

TABLE V: Test Accuracy of GCN Model

Model	Test Accuracy
GraphCNN_VGG16	0.713198
GraphCNN_Densenet121	0.642132
GraphCNN_Resnet18	0.715736

VIII. Conclusion and Future Scope

They demonstrate the effectiveness of GATs in harnessing spatial dependencies in MRI images to accurately classify brain tumor. The synergy between GNNs and CNNs, especially when combined with attention processes, improves the model's ability to detect subtle patterns and fluctuations in tumor features.

The choice of backbone architecture is critical in deciding the model's performance, with VGG-16 emerging as the best performer in the tests. However, DenseNet121 and ResNet-18 both perform well, demonstrating GATs' adaptability in supporting various network architectures. Future work involves refining and optimizing the algorithms and exploring the optimization techniques, data augmentation strategies. Collaborating with medical researchers for more extensive dataset which would help in making models more robust to general data and integrating it with existing hospital systems.

References

[1] Ghassemi, N., Shoeibi, A., and Rouhani, M. "Deep neural network with generative adversarial networks pre-training for brain tumor classification based on MR images." Biomed. Signal Process. Control, vol. 57, p. 101678, 2020.processing (ICCSP), pp. 0018-0022. IEEE, 2018.

[2] Alzubaidi, L. et al. "MedNet: Pre-trained convolutional neural network model for medical imaging tasks." arXiv, 2021. eprint: 2110.06512. https://arxiv.org/abs/2110.06512

[3] Varthakavi, Sai Sasank, Devisetty Rohith Prasanna Babu, Amsitha MB, and Sasi Jyothirmai Bonu. Analysis of Classification Algorithms for Brain Tumor Detection. No. 1810. EasyChair, 2019.

[4] Krishnan, Rohith, P. G. Gokul, Gopikrishnan Sujith, T. Anjali, and S. Abhishek. "Enhancing Brain Tumor Diagnosis: A CNN-Based Multi-Class Classification Approach." In 2024 IEEE International Conference on Interdisciplinary Approaches in Technology and Management for Social Innovation (IATMSI), vol. 2, pp. 1-6. IEEE, 2024.

[5] Jeena, Kottarapat, Cheripelil Abraham Manju, Koythatta Meethalveedu Sajesh, G. Siddaramana Gowd, Thangalazhi Balakrishnan Sivanarayanan, Deepthi Mol C, Maneesh Manohar, Ajit Nambiar, Shantikumar V. Nair, and Manzoor Koyakutty. "Brain-tumor-regenerating 3D scaffold-based primary xenograft models for glioma stem cell targeted drug screening." ACS Biomaterials Science Engineering 5, no. 1 (2019): 139-14

[6] Çinar, A., and Yildirim, M. "Detection of tumors on brain MRI images using the hybrid convolutional neural network architecture." Med. Hypotheses, vol. 139, p. 109684, 2020.

[7] Mehrotra, R., Ansari, M. A., Agrawal, R., and Anand, R. S. "A transfer learning approach for AI-based classification of brain tumors." Mach. Learn. Appl., vol. 2, p. 100003, 2020.

[8] Raza, A. et al. "A hybrid deep learning-based approach for brain tumor classification." Electronics, vol. 11, no. 7, p. 1146, 2022.

[9] Dehkordi, A. A., Hashemi, M., Neshat, M., Mirjalili, S., and Sadiq, A. S. "Brain tumor detection and classification using a new evolutionary convolutional neural network." arXiv, 2022. eprint: 2204.12297.

[10] Ge, C., Gu, I. Y. H., Jakola, A. S., Yang, J. "Enlarged training dataset by pairwise GANs for molecular-based brain tumor classification." IEEE Access, 8, 22560–22570 (2020).
[11] Deepak, S., and Ameer, P. M. "Brain tumor classification using deep CNN features via transfer learning." Comput. Biol. Med., vol. 111, p. 103345, 2019.
[12] Sajjad, M. et al. "Multi-grade brain tumor classification using deep CNN with extensive data augmentation." J. Comput. Sci., vol. 30, pp. 174182, 2019.
[13] Varthakavi, Sai Sasank, Devisetty Rohith Prasanna Babu, Amsitha MB, and Sasi Jyothirmai Bonu. Analysis of Classification Algorithms for Brain Tumor Detection. No. 1810. EasyChair, 2019.
[14] Kavitha, K. R., Amritha S. Nair, and Vishnu Narayanan Harish. "Detection Of Brain tumor Using Deep Convolutional Network." In 2023 4th IEEE Global Conference for Advancement in Technology (GCAT), pp. 1-6. IEEE, 2023.
[15] Díaz-Pernas, F. J., Martínez-Zarzuela, M., Antón-Rodríguez, M., and González-Ortega, D. "A deep learning approach for brain tumor classification and segmentation using a multiscale convolutional neural network." Healthcare, vol. 9, no. 2, p. 153, 2021.